CHAPTER 153

AN OVERVIEW OF THE BRITISH BEACH AND NEARSHORE DYNAMICS (B-BAND) PROGRAMME.

[1]M.A. Davidson, [2]P.E. Russell, [2]D.A. Huntley,
[3]J. Hardisty and [4]A. Cramp.

ABSTRACT

The British Beach And Nearshore Dynamics (B-BAND) programme is a three year collaborative research project aimed at improving understanding of surf zone sediment transport processes. Field studies were carried out on dissipative, intermediate and reflective beaches during both neap and spring tides (tidal range up to 9m), and during storm wave ($H_b > 3$m) conditions.

The field research system comprises up to 7 pressure transducers (PT's), 11 electromagnetic current meters (EMCM's) and 12 optical backscatter sensors (OBS's). The focal point of the instrument array was a 1600m^2 box which was instrumented at each corner and designed to allow the calculation of alongshore and cross-shore suspended sediment fluxes through the box.

The largest sediment transport rates (up to 0.6 kgm^{-2}s^{-1}) occurred in the inner surf zone of the dissipative beach during storm conditions and showed strong offshore-directed sand transport at infragravity frequencies. The extent to which infragravity oscillations developed was seen to vary inversely with the degree of beach reflectivity, and directly with the incident breaker height. Sediment transport patterns often exhibited strong tidal asymmetry, attributed to the effects of beach de-watering and to a lag between hydrodynamics and bedform alteration.

---

[1] Dept. of Civ. & Structural Eng., Univ. of Plymouth, UK. [2] Institute of Marine Studies, Univ. of Plymouth. UK. [3] School of Geography, The Univ., Hull, UK. [4] Marine Geosciences Group, Geology Dept., Univ, of Cardiff, UK.

INTRODUCTION

Many large multi-institutional field studies examining nearshore processes, using dense arrays of fast response sensors, have taken place over the last decade. These include; the Nearshore Sediment Transport Study (NSTS) on the west coast of the USA (Seymour, 1989), the Natural Environmental Research Council (NERC) project in Japan (Horikawa, 1987), the Canadian Coastal Sediment Transport Study (C^2S^2, Willis, 1987), and the DUCK experiments (eg. DUCK82, Mason *et al.*, 1984 and SUPERDUCK86, Martens and Thornton, 1987) carried out on the east coast of the USA.

These studies have substantially improved the understanding of surf zone hydrodynamics. However, progress in understanding the sediment response has been disappointing (Battjes, 1988). This is partially due to the fact that many of the field experiments have taken place on microtidal and mesotidal beaches with complex profiles and bedforms. Also our knowledge of the bedload phase is limited, because devices capable of obtaining high frequency bedload measurements on natural beaches are still under development (Hardisty, 1991).

The British Beach And Nearshore Dynamics (B-BAND) programme (1990-93) (Russell *et al.*, 1991) is a UK-based multi-institutional project. Its aim is to improve knowledge of surf zone sediment dynamics and shoreline evolution through the application of dense arrays of fast response sensors and detailed measurements of the associated shoreline change. Data was collected from high energy macrotidal beaches, which typically have a broad tidal and intertidal sand flat of shallow linear slope almost completely devoid of bedforms. A complementary low energy UK field study (Bedform And Suspension EXperiments, BASEX, cf. Osborne and Vincent, this volume) is examining small-scale suspension processes over rippled beds seaward of the surf zone, using acoustic suspension profiling techniques.

This contribution provides an overview of the environments sampled during the B-BAND experiment, the techniques used and some of the results obtained.

FIELD STUDIES

The field research system comprised up to 7 pressure transducers (measuring depth and surface waves), 11 electromagnetic current meters (measuring bi-directional horizontal near-bed currents) and 12 optical backscatter sensors (measuring suspended sediment concentrations, SSC's). The focal point of the array was a $1600m^2$ box which was instrumented at each corner (Figure 1). These corner stations typically consisted of 3 EMCM's at heights of 0.10, 0.25, and 0.63m above the bed, 3 OBS's at heights of 0.04, 0.10, and 0.25m above the bed, and a single PT. This arrangement was designed to allow the calculation of both the alongshore and cross-shore suspended sediment fluxes through the box, whilst standard beach profiling techniques in conjunction with a dense array of depth of disturbance rods provided estimates of net erosion and accretion within the box over a tidal cycle. Additionally, a cross-shore array of 5 PT's permitted measurements of wave shoaling characteristics across the profile. Self Generated Noise (SGN) and Ultrasonic Current Meter (UCM) sensors were also deployed to estimate bedload sediment transport and 3 dimensional current flow close to the bed, respectively.

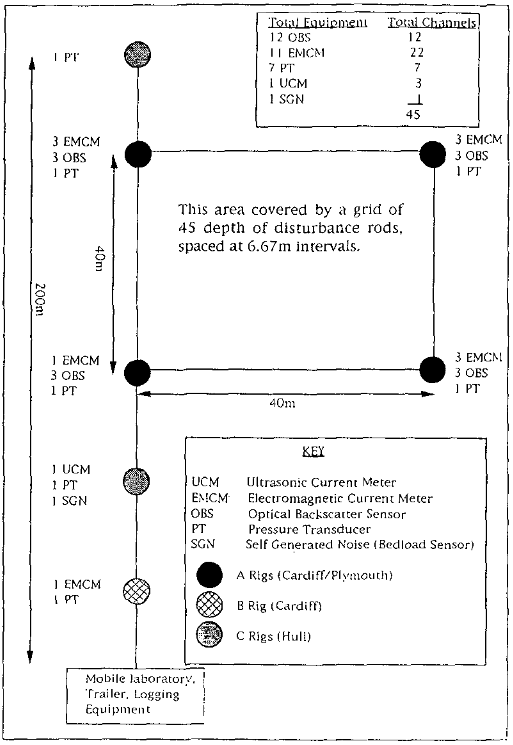

Figure 1: Generalised B-BAND field set-up.

The sensors were secured by burying their mountings below the sand surface, and the 200m cables were buried back up to the logging equipment in the mobile laboratory at the head of the beach. The large tidal range on these macrotidal beaches allowed a profile of measurements to be obtained through and beyond the surf zone over a tidal cycle. Care was taken to ensure that the instrument mountings were buried in excess of 10cm below the sediment-water interface so as to prevent self-suspension by the rigs themselves. Depth of disturbance measurements indicated that maximum disturbance depths were less than 10cm over a tidal cycle. The OBS's were mounted to a slender (3mm diameter) stem which protruded out of the sediment-water interface from the subsurface mountings. No signs of scour were observed around these stems.

Signals were low-pass filtered (cut-off frequency = 1Hz) and digitised at a rate of 2Hz on a personal computer. Each data run was 17.07 minutes in duration giving 2048 data points per channel. Data were recorded continuously from just after low water on the flooding tide to just before low water on the ebbing tide. Beach profile and depth of disturbance measurements were obtained during each low water period.

Field investigations were carried out at three macrotidal beach sites: Llangennith, South Wales; Spurn Head, North East England and Teignmouth, South West England (Figure 2). Following Wright and Short's (1984) morphodynamic classification of beaches, these sites will hereafter be referred to as the dissipative, intermediate and reflective beaches respectively.

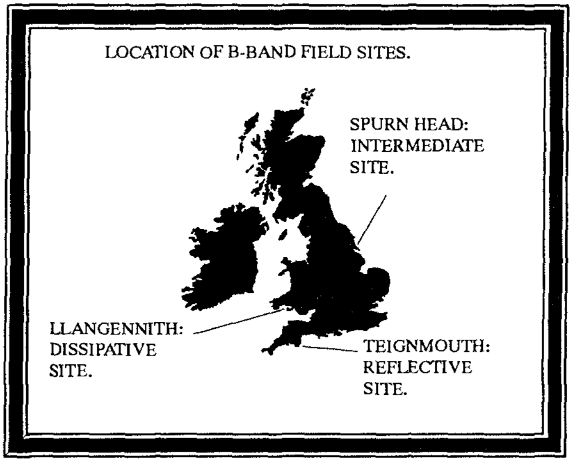

Figure 2: B-BAND field sites.

The dissipative beach is a 10km long, high energy beach with a shallow concave beach profile (gradient = 0.014-0.020) consisting of fine to medium grained quartz sands (D_{50}= 0.21mm). The wave climate on this exposed west facing beach is a mixture of high energy Atlantic swell approaching from the WSW, and locally generated wind waves driven by the prevailing W and SW winds. The low beach gradient, high energy waves and large (up to 9m) tidal range combine to produce both broad surf (up to 350m wide) and intertidal (up to 500m wide) zones.

The intermediate beach site is located near the end of a 5km long spit and faces into the North Sea. The prevailing wave climate is milder than that of the dissipative beach, but the coast is exposed to occasional violent storm waves which approach obliquely from the north-east and can produce plunging breakers with heights in excess of 3m. The beach profile consists of a steep high tide beach (gradient = 0.0975) comprised of fine to medium gravels and a shallow sloping (gradient = 0.023) low tide terrace consisting of a lens of well sorted, medium quartz sands (D_{50}= 0.35mm) overlying boulder clays. Strong (up to 1m/s) rectilinear tidal currents (tidal range = 3 to 6m) run parallel to the coast flowing in a south-westerly direction on the flood and north-easterly direction during the ebb. These currents exert a significant dynamical effect even within the surf zone.

The reflective beach site faces south-east into the English Channel and is consequently sheltered from swell waves generated in the Atlantic Ocean. The local wave climate is dominated by infrequent periods of wind-driven waves from the east. The beach profile is headed at its shoreward extent by a vertical sea wall. The upper profile adjacent to the sea wall is convex and the lower profile seawards of the neap low tide level is slightly concave. The beach is comprised of medium

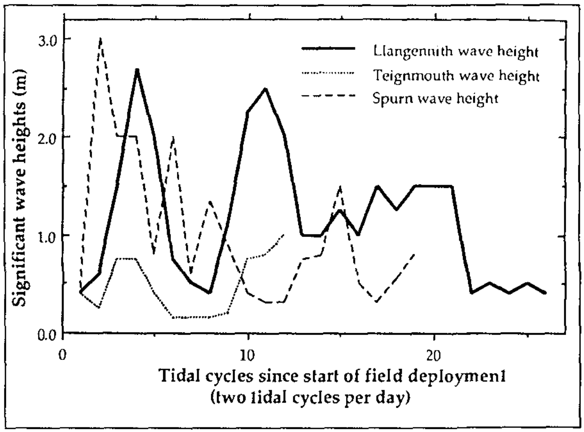

Figure 3: Wave height variation during the B-BAND experiments.

quartz sand (D_{50}= 0.24mm). Due to the steep beach profile (gradient = 0.067 to 0.142) the intertidal zone at the reflective beach is comparatively narrow (<70m) in spite of the large (up to 6m) tidal range in this area.

A wide range in incident wave conditions were experienced during each field deployment (Figure 3). Measurements were obtained during both calm conditions and through two storm events ($H_{1/3}$= 2 to 3m) at the dissipative beach. The start of the intermediate beach experiment was marked by the largest storm in 3 years ($H_{1/3}$ > 3m) which breached the sand spit leaving it isolated from the mainland at high water. Wave energy levels were much lower during the reflective beach experiment. However, two periods of high wave energy for the locality did occur during the experiment (tides 3-4 and 11-12) when significant wave heights were between 0.5 and 1m.

RESULTS

The following discussion of the time series data is subdivided into hydrodynamics, sediment suspension, sediment transport and beach response. Further divisions are made where appropriate into oscillatory and steady components.

Hydrodynamics. a) Oscillatory flows:

The typical cross-shore pattern for the distribution of hydrodynamic variance observed on all the beaches sampled irrespective of the degree of profile reflectivity is shown in Figure 4. This example, recorded at the intermediate beach, shows the variation of the cross-shore current velocity spectrum with offshore distance. The energy distribution with offshore distance of all the principal components (incident, incident harmonics and infragravity components) of the spectrum appears to conform to current theory (cf. Ursell, 1952; Wright *et al.*, 1982). The shorewards decay of incident wave energy and its associated harmonics within the surf zone is accompanied by a simultaneous increase in energy within the infragravity band.

Although this basic pattern for the distribution of hydrodynamic variance is

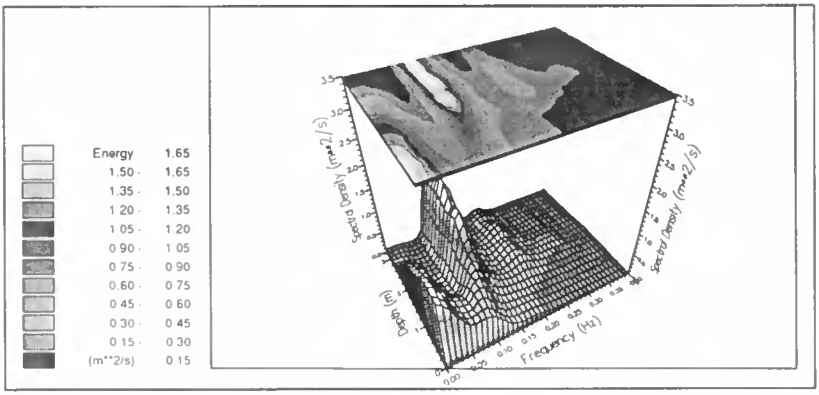

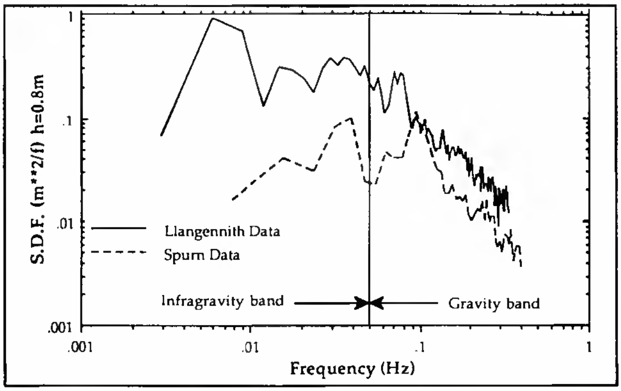

Figure 4: (above) Variation in the cross-shore current spectrum with offshore distance, (intermediate beach).

Figure 5: A comparison of cross-shore current spectra from the intermediate and dissipative beaches.

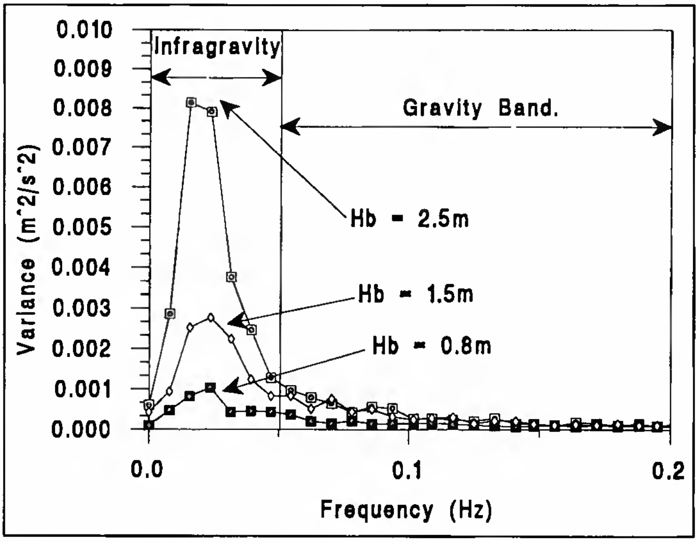

Figure 6: Infragravity response to incident wave forcing. (results from the inner surf zone of the dissipative beach).

common to all the beaches occupied, the relative importance of the principal components of the spectrum varies depending on the reflectivity of the environment. Two cross-shore current velocity spectra from the intermediate and dissipative beaches recorded in equivalent water depths (h = 0.8m) during comparable incident wave conditions ($H_{1/3}$ = 2.5m) are presented in Figure 5. Hydrodynamic spectra recorded at the dissipative beach are strongly dominated by oscillations at infragravity frequencies, whilst at the more reflective environment, incident wave motion dominates the spectrum.

Results obtained in this experiment have supported the findings of other researchers (cf. Holman, 1981) who have demonstrated that, for a given beach, the shoreline infragravity energy levels are linearly related to incident wave height. This proportionate response of the infragravity band with increased incident wave forcing is demonstrated in Figure 6 (and in Huntley *et al.*, 1992). However, observations on beaches of varying reflectivity indicate that levels of long wave energy are not simply a function of the incident wave climate and that beach slope is an important factor which must be considered when predicting infragravity energy within the nearshore zone.

b) Mean Flows: Longshore currents.

The typical patterns for the variation in longshore current velocity with offshore distance through and beyond the surf zone at the intermediate and reflective sites are illustrated in Figures 7a and b. These figures show the effect of both the temporal variation in the tidal component and the spatial variation in the wave driven flow. The wave driven longshore flow in both cases is negative (to the south), enhancing tidal flows on the flood tide and opposing tidal flows during the ebb. The variation in the magnitude of the wave driven component conforms qualitatively to the theoretical profile of Longuet-Higgins (1970) which predicts low velocities within the inner/outer surf zone and a mid-surf maximum.

Observations indicated that the net longshore current was the resultant of wave and tidally driven components. The relative importance of these components varied with tidal state, cross-shore location and beach reflectivity.

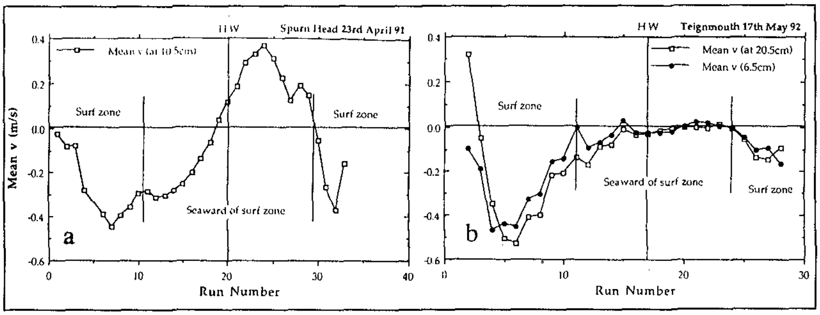

Figure 7a, b: Variations in the mean longshore current with run number (depth) for a) the intermediate beach and b) the reflective beach.

The tidal component was found to be particularly important in coastal regions where dominant tidal flows run parallel to the coast at the intermediate and reflective beach sites. At the dissipative beach, mean longshore flows were found to be weak due to both the low angle of wave attack and the prevalent direction of tidal flow which is perpendicular to the shoreline.

Mean Flows: Cross-shore currents.

Comparative plots for the cross-shore component of flow are shown in Figure 8a and b. The pattern of flow is very repeatable both temporally within a given environment and at different sites. Within the surf zone, a strong (0.2m/s) near-bed offshore flow (undertow) is evident. On the intermediate beach there is also a weak (0.05m/s) near-bed onshore flow seawards of the surf zone. These results suggest a convergence in the steady near-bed cross-shore flow towards the break point. Similar results have been obtained by other workers, (eg. Bailard, 1987).

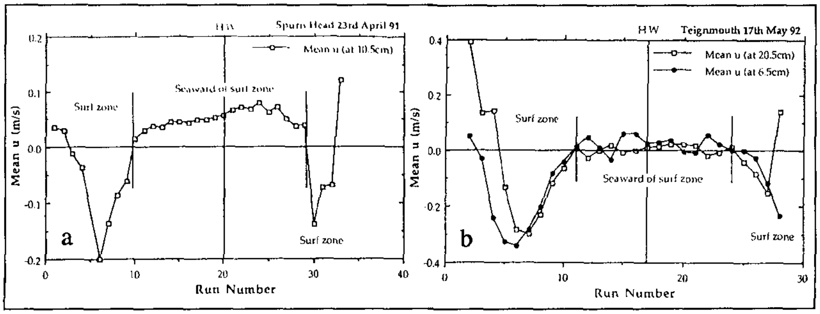

Figure 8a, b: Variation in mean cross-shore current velocity with run number (depth) at a) the intermediate beach and b) the reflective beach.

A second feature of the mean cross-shore flow field commonly observed within the surf zone is an onshore near-surface flow. This is particularly noticeable in the readings obtained from the upper current meters just prior to them coming out of the water. In some cases there is evidence for a vertical flow reversal (see for example runs 2, 3 and 28, Figure 8b) with onshore flow close to the surface and offshore flow at depth. Similar results have been presented by Wright *et al.* (1982) and Bailard (1987).

Sediment Suspension.

Typical SSC and cross-shore velocity time series measured at the intermediate and dissipative beach are shown in Figures 9a and b respectively. These data were collected in similar water depths (h = 0.4-0.45m) within the inner surf zone during similar (incident) wave conditions. The suspension characteristics shown in Figure 9a are typical of those observed on both the intermediate and reflective beaches, with suspension events generally occurring on each wave cycle at incident

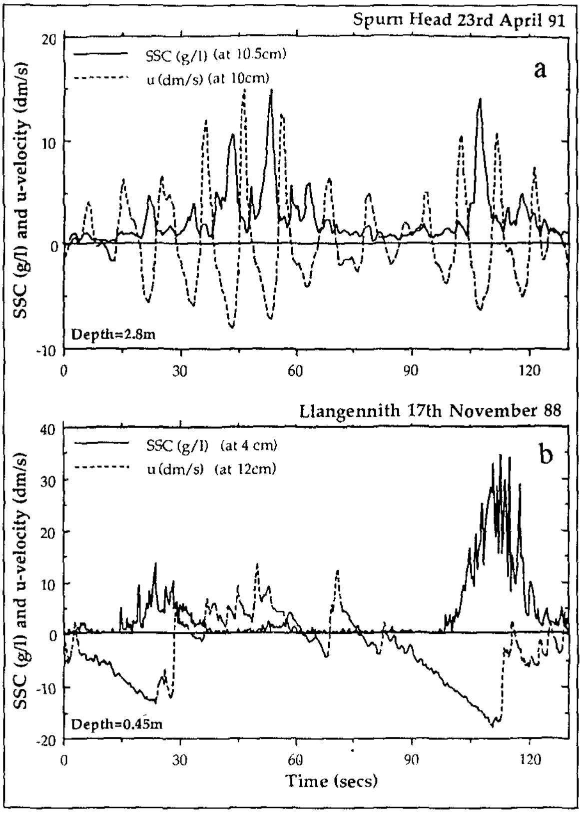

Figure 9a, b: Typical cross-shore current and SSC time series measured in the inner surf zone on a) the intermediate beach and b) the dissipative beach.

wave frequencies and the associated harmonics, with some secondary modulation at infragravity wave frequencies. Conversely, on the dissipative beach, suspension events are long lived (30 to 60s), dense (30 to 50g/l) and closely correlated with prolonged offshore flows at infragravity frequencies.

Several of the B-BAND data sets show a profound tidal asymmetry in both the steady and oscillatory sediment suspension components. Examples of this phenomenon recorded at the intermediate beach during two different tides are shown in Figures 10a to d. These plots illustrate tidal asymmetry in the suspension data at different heights in the water column (top, middle and bottom OBS sensors), and at different spatial locations on the beach (eg rigs A3 and A2) in both the mean (Figures 10a and c) and oscillatory components (Figures 10b and d). The main reasons for the observed tidal asymmetry are thought to be de-watering of the beach during the ebb and a time-lag in bed-form response to changing hydrodynamic conditions (Davidson *et al.*, in press).

SEDIMENT TRANSPORT.

1) Cross-shore

Co-spectral techniques were extensively employed to examine the magnitude and direction of fluctuating sediment fluxes with frequency at different locations.

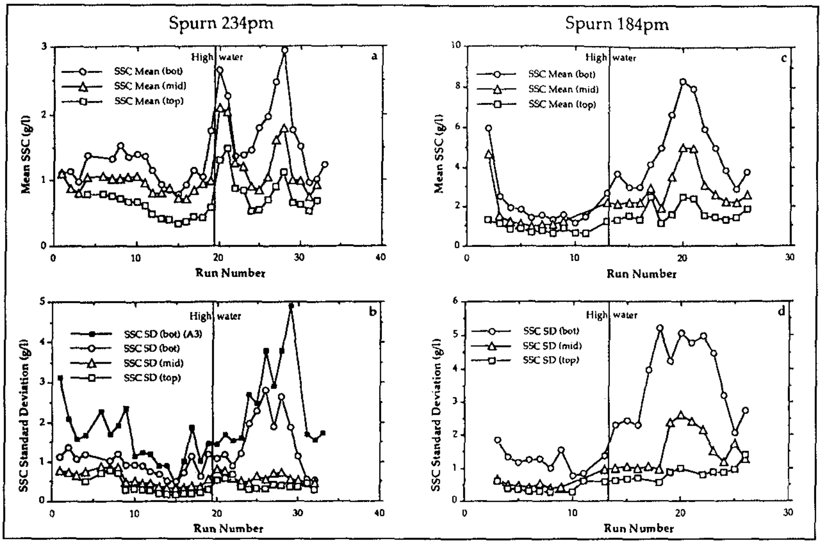

Figure 10a, b, c, d: Variation in steady and oscillatory SSC with run number (offshore distance) and height above the bed (intermediate beach).

These results have supported earlier research carried out on beaches of low tidal range. For example, weak onshore transport at incident wave frequency was found seaward of the surf zone (eg. Huntley and Hanes, 1987, and Figure 11). Conversely, within the surf zone, offshore sediment fluxes at infragravity frequencies were much greater in magnitude than the corresponding onshore transport at incident wave frequencies (eg. Russell, 1990, Figure 12 from the dissipative beach, and Figure 13 from the intermediate beach).

However, other processes can alter this basic pattern. For example, the co-spectrum in Figure 14 illustrates strong offshore transport at incident wave frequencies over a rippled bed seawards of the surf zone at the intermediate site. This reverse transport at

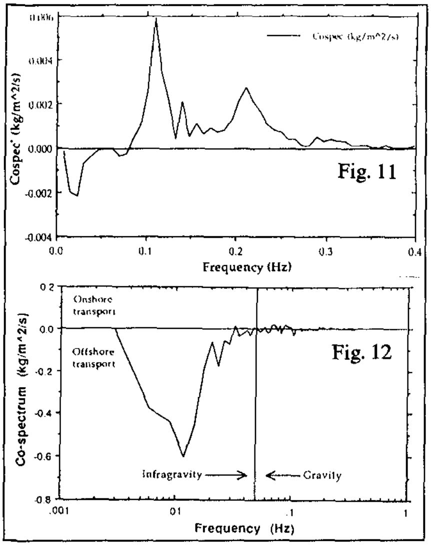

Figures 11 and 12: Cross-shore current, SSC co-spectra.

incident wave frequencies over rippled beds has been noted by other workers (cf. Dingler and Inman, 1976).

2) Longshore.

In the longshore direction, the oscillatory transport contributions were negligible since the fluctuating component of longshore velocity and SSC were uncorrelated. The steady (both wave-driven and tidally modulated) flows dominated the longshore transport of sediment.

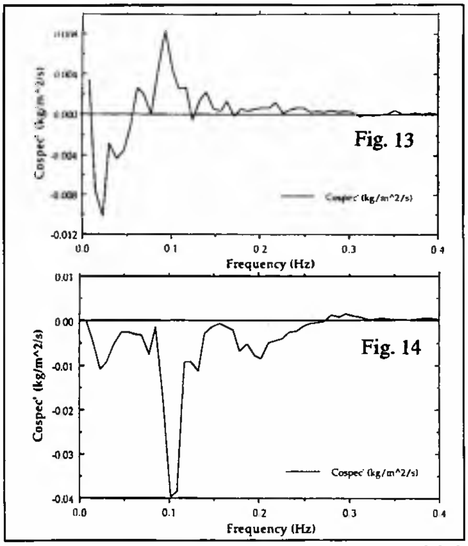

Figure 13 and 14: Cross-shore current, SSC co-spectra. (13) Inner surf zone. (14) Over ripples (14).

BEACH RESPONSE.

The sequence of beach profiles collected during the dissipative beach deployment are illustrated in Figure 15. This data has been re-plotted in Figure 16 as a 2-dimensional plan to illustrate the change in beach level between consecutive profiles, so that areas of erosion and accretion can be readily observed. The classic pattern of offshore transport from a berm to an offshore bar is observed during the storm wave conditions at the start of the experiment (profile numbers 1-4), followed by a subsequent return of sand from the bar to the berm during small swell wave conditions later in the deployment (profile numbers 8-11).

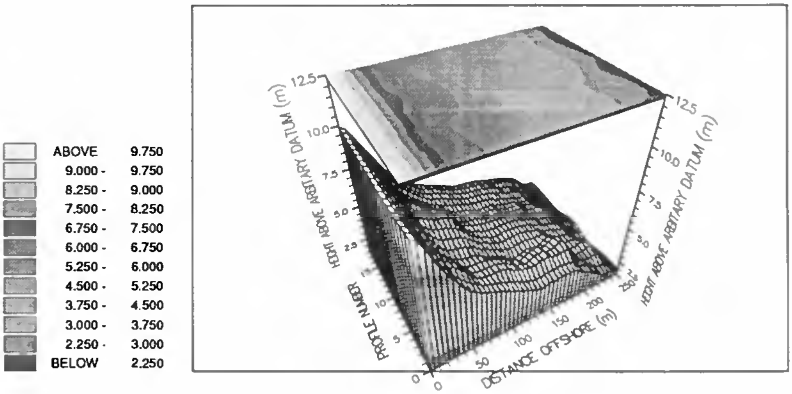

Figure 15: Beach profile evolution (Llangennith).

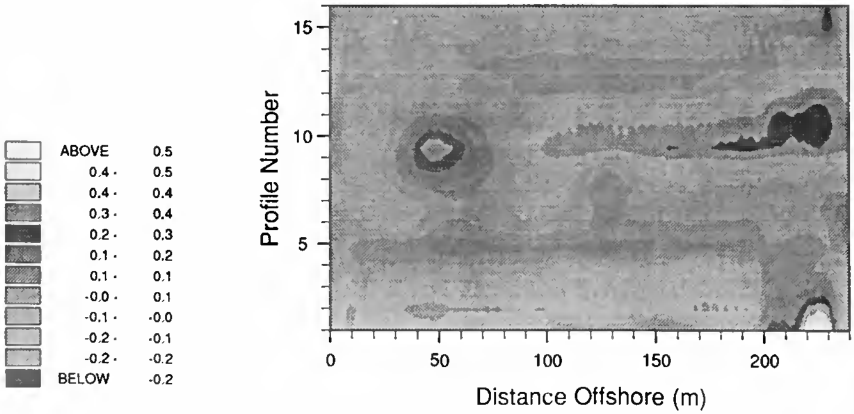

Figure 16: Beach changes during the dissipative beach experiment.

Depth of disturbance (DOD) measurements gave detailed bed level changes inside the box averaged over a tidal cycle. A typical result is illustrated in Figure 17. However, no reliable quantitative comparisons could be made between the measured bed level changes in the box and sediment fluxes measured at fixed heights by the sensors. This is because of the inability of the suspension (OBS) and velocity (EMCM) sensors to measure sediment suspension either within the swash zone or within the bottom boundary layer. Hence, the calculation of accurate time- and depth-integrated sediment fluxes over a tidal cycle was not possible. The accurate measurement of the total load sediment transport rates in the surf zone awaits further development of instruments which are capable of obtaining reliable fast response concentration and velocity profiles which extend well into the bottom boundary layer, and are also capable of measuring within the swash zone.

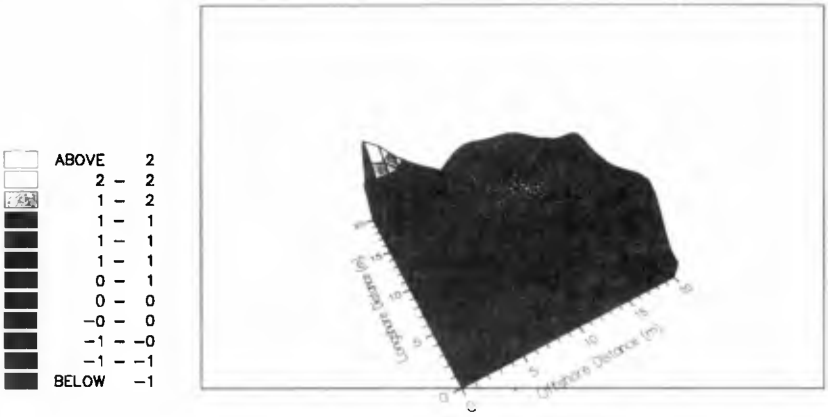

Figure 17: Bed level changes within the box.

CONCLUSIONS.

Results obtained using dense arrays of PT's, EMCM's and OBS's are invaluable for furthering our understanding of hydrodynamic and sediment transport processes on natural beaches. Results of particular interest so far include:

i) The tidal asymmetry, affecting sediment transport processes on macrotidal beaches.

ii) The relative importance of steady flows, long waves (surf beat) and incident waves to the total sediment transport rates in the surf, breaker and offshore zones and on beaches with differing slopes.

iii) The relationship between infragravity response and incident wave forcing. The magnitude of infragravity perturbations are inversely related to beach reflectivity and directly related to incident breaker height.

iv) The magnitude and phase relationships between cross-shore flows and sediment suspension with height above the bed.

v) Assessing the reliability of fast response sensors in the prediction of the divergence of sediment across a given area.

Work is continuing on analysing the vast (325 Mbyte) B-BAND data set, with particular emphasis on the influence of mean flows, reflection from coastal structures, infragravity sediment transport and beach response.

ACKNOWLEDGEMENTS

The B-BAND experiment is being funded by the Natural Environment Research Council (NERC) (UK) research grant GR3/7128. The post doctoral research associates, Mark Davidson and Paul Russell would like to thank the Welsh Office and the NERC respectively for supporting their work on this project. The authors would also like to extend their thanks to Gareth Lloyd and Steven Jacques for assistance with drafting the figures.

REFERENCES

Bailard, J., 1987, Surf zone wave velocity moments, Proc. Coastal Hydrodynamics, ASCE, 328-342.

Davidson, M.A., P.E. Russell, D.A., Huntley and J. Hardisty, in press, Tidal asymmetry in suspended sand transport on a macrotidal intermediate beach. Mar. Geol.

Dingler, J.R. and D.L. Inman, 1976, Wave formed ripples in nearshore sands, Proc. 15th Coastal Eng. Conf., ASCE, 2109-2126.

Guza, R.T. and E.B. Thornton, 1982, Swash oscillations on a natural beach, J. Geophys. Res., 87, 483.

Hardisty, J., 1991, Bedload transport under low frequency waves, Proc. Coastal Seds. '91, ASCE, 726-733.

Holman, R.A., 1981, Infragravity energy in the surf zone, J. Geophys. Res., 86(7), 6442-6450.

Horikawa, K., 1987, Nearshore dynamics and coastal processes - theory, measurement and predictive models, Univ. of Tokyo Press, 515pp.

Huntley, D.A. and Hanes, D.M., 1987, Direct measurement of suspended sand transport, Proc. Coastal Seds.,' 87, ASCE, 723-737.

Huntley, D.A., M.A. Davidson, P.E. Russell, Y. Foote and J. Hardisty, in press, Long waves and sediment movement on beaches; recent observations and implications for modelling, J. Coastal Research.

Longuet-Higgins, M.S., 1970, Longshore currents generated by obliquely incident sea waves, 2, J. Geophys. Res., 75, no. 33, 6790-6801.

Martens, D.E. and E.B. Thornton, 1987, Nearshore zone monitoring system. Proc. Coastal Hydrodynamics, ASCE, 579-588.

Mason, C., A.H. Salenger, R.A. Holman, and W.A. Birkemeier, 1984, DUCK82 - A coastal storm processes experiment, Proc. 19th Coastal Eng. Conf., ASCE, 1913-1928.

Osborne, P.D. and C.E. Vincent, in press, Timescales of bed response in a low energy surf zone. Proc. 23rd Coastal Eng. Conf., ASCE.

Russell, P.E., 1990, Suspended sand transport on a high energy dissipative beach, Unpub. Ph.D. Thesis, Univ. of Wales, 318pp.

Russell, P.E., M.A. Davidson, D.A. Huntley, A. Cramp, J. Hardisty and G. Lloyd, 1991, The British Beach And Nearshore Dynamics (B-BAND) programme, Proc. Coastal Seds '91, ASCE, 371-384.

Seymour, R.J., 1989, Nearshore sediment transport, Plenum Press, NY, 450pp.

Ursell, F., 1952, Edge waves on a sloping beach, Proc. Roy. Soc. London, 214, 79-97.

Willis, D.H., 1987, The Canadian Coastal Sediment Transport Study: An overview, Proc. Coastal Sediments '87, ASCE, 682-693.

Wright, L.D., R.T. Guza and A.D. Short, 1982, Dynamics of a high-energy dissipative surf zone, Mar. Geol., 45, 41-128.

Wright, L.D. and Short, A.D., 1984, Morphodynamic variability of surf zones and beaches: a synthesis, Mar. Geol., 56, 93-11.